Journal of Alloys and Compounds 579 (2013) 468–472

Contents lists available at SciVerse ScienceDirect

Journal of Alloys and Compounds

journal homepage: www.elsevier.com/locate/jalcom

Electronic and optical properties of Cu_2ZnGeX_4 (X = S, Se and Te) quaternary semiconductors

Dongguo Chen *, N.M. Ravindra

Department of Physics, New Jersey Institute of Technology, Newark, NJ 07102, USA

ARTICLE INFO

Article history:
Received 1 March 2013
Received in revised form 1 June 2013
Accepted 9 June 2013
Available online 18 June 2013

Keywords:
Cu_2ZnGeX_4(*X* = S, Se, Te)
Band structure
Density of states
Dielectric function
Refractive index
Absorption

ABSTRACT

The electronic structures and optical properties of Cu_2ZnGeS_4, $Cu_2ZnGeSe_4$ and $Cu_2ZnGeTe_4$ in kesterite and stannite structures are investigated using first-principles calculations. The critical points in the optical spectra are assigned to the interband transitions according to the calculated band structures. The trends in the variation of the electronic and optical properties are discussed with respect to the crystal structure and the anion atomic number. Our calculated properties, such as, lattice constants, optical transitions, refractive index and dielectric constants are compared to the available experimental data and good agreement is obtained.

1. Introduction

The I_2–II–IV–VI_4 series of quaternary chalcogenide semiconductors have been of broad interest for their potential applications as photovoltaic absorbers [1–5], optoelectronic and thermoelectric materials [6–8]. For instance, Cu_2ZnSnS_4 based thin film solar cells have reached a conversion efficiency over 6.7% [4]. Recently, a non-vacuum, slurry-based coating method and particle-based deposition, enabled the fabrication of $Cu_2ZnSn(S, Se)_4$ devices with over 9.6% efficiency [6]. Compared to the conventional $CuIn_{1-x}Ga_xSe_2$ absorbers, Cu_2ZnSnS_4 and $Cu_2ZnSnSe_4$ compounds only contain abundant, inexpensive and nontoxic elements and their band gaps are close to 1.5 eV, which is ideal for solar cell applications.

The wide applications increase the interest of studying many other members in the I_2–II–IV–VI_4 family, such as, the Ge-compounds: Cu_2ZnGeS_4, $Cu_2ZnGeSe_4$ and $Cu_2ZnGeTe_4$. In experiment, the physical properties [9–13], such as, crystal orderings and lattice constants of these compounds have been studied using X-ray diffraction method. Transmission [14] and absorption measurements [15] are conducted to study the band gaps. Recently, the optical constants of Cu_2ZnGeS_4 have been reported by ellipsometry measurements [16]. In theoretical work, the structural and electronic properties of some compounds have been studied using first-principles calculations [17,18]. However, the optical properties of these compounds have not been systematically addressed yet.

In this paper, we investigate the electronic and optical properties of Cu_2ZnGeX_4 (X = S, Se and Te) quaternary compounds in tetragonal kesterite-type (KS) structure (space group $I\bar{4}$) and stannite-type (ST) structure (space group $I\bar{4}2m$) [19], through first-principles calculations within density functional theory (DFT). We first calculate the electronic structures and density of states because it is known that the structures in the optical spectra are directly related to the band structure of the material itself. Then, we present the optical properties, including the dielectric function, refractive index, optical reflectivity and absorption spectra. The trends in the variation of the electronic and optical properties with the crystal structure and the group VI anion atomic number are explored qualitatively.

2. Computational method

The calculations are performed with the Cambridge serial total energy package (CASTEP) code, which is based on the density functional theory using a plane-wave pseudopotential method [20,21]. We use the generalized gradient approximation (GGA) in the scheme of Perdew–Burke–Ernzerhof (PBE) to describe the exchange–correlation functional [22]. The ion–electron interaction is modeled by Vanderbilt ultrasoft pseudopotential [23]. We choose the energy cutoff to be 400 eV, and the Brillouin-zone sampling mesh parameters for the *k*-point set is $5 \times 5 \times 5$ for all the cases. The total energy is converged to 1×10^{-6} eV/atom in the self-consistent calculation. In the structural optimization process, the energy change, maximum force, maximum stress and the maximum displacement tolerances are set to be 2×10^{-5} eV/atom, 0.05 eV/Å, 0.2 GPa, and 0.001 Å, respectively.

* Corresponding author. Tel.: +1 19732209362.
E-mail address: dc74@njit.edu (D. Chen).

0925-8388/$ - see front matter © 2013 Elsevier B.V. All rights reserved.
http://dx.doi.org/10.1016/j.jallcom.2013.06.048

Table 1
Calculated lattice constant a and c, band gap before and after correction E_g^{GGA}, E_g, critical point threshold energy E_{1A} and E_{1B}, and static optical constants. Experimental data Refs. [9–16] are listed for comparison, whereas "—" means no experimental data are currently available.

	Cu_2ZnGeS_4			$Cu_2ZnGeSe_4$			$Cu_2ZnGeTe_4$		
	KS	ST	Exp.	KS	ST	Exp.	KS	ST	Exp.
a (Å)	5.264	5.328	5.270, 5.342	5.602	5.583	5.606, 5.610	6.102	6.094	5.954, 5.999
c (Å)	10.843	10.741	10.509, 10.516, 10.540	11.259	11.325	11.04	12.126	12.220	11.848, 11.918
E_g^{GGA} (eV)	0.76	0.47	–	0.06	−0.22	–	−0.24	−0.50	–
E_g (eV)	2.43	2.14	2.15, 2.28, 2.04	1.60	1.32	1.63, 1.52, 1.29	0.81	0.55	–
E_{1A} (eV)	2.99	2.66	2.85, 2.87, 2.88	2.35	1.838	–	1.139	0.659	–
E_{1B} (eV)	4.10	3.83	4.03, 4.28, 4.34	3.58	3.171	–	2.214	1.793	–
n_0	2.58	2.61	–	2.90	3.00	–	3.73	4.23	–
ε_0	6.68	6.80	–	8.25	9.01	–	13.89	17.93	–
ε_∞	0.48	0.49	0.47, 0.49, 0.76	0.51	0.53	–	0.50	0.54	–

3. Results and discussion

The calculated properties of Cu_2ZnGeS_4, $Cu_2ZnGeSe_4$ and $Cu_2ZnGeTe_4$ of KS and ST structures are listed in Table 1. Together listed are the available experimental values for comparison. We noticed that many of the experimental reports [9–13] on these compounds claim that the synthesized samples have ST structure. For example, Parasyuk and co-workers [11,13] synthesized Cu_2ZnGeS_4, $Cu_2ZnGeSe_4$ and $Cu_2ZnGeTe_4$ samples from high-purity elements and determined their crystal constants by X-ray diffraction. They claim that all the three samples crystallize in the ST structure. However, the calculation finds that KS is the ground state structure due to the lower formation energy. It is believed that this discrepancy arises from the fact that the experimental synthesis of the compounds is not carried out at equilibrium conditions. In fact, more recent experiments have found that the I_2–II–IV–VI_4 compounds favor KS as the ground state structure which support the theoretical prediction [3,24]. We find that our calculated structural parameter $c/2a$ is in general larger than unity, for ST structure, while the experimental values [11,13] show that it is less than unity. We believe that this discrepancy between the experiments and our calculations is caused by the fact that the similarity of Cu and Zn atoms leads to the cation disorder in their experimental structures. Because the atomic numbers of Cu, Zn and Ge are close in the periodic table, experimentally, it is very difficult to detect the cation disorder by X-ray diffraction. In fact, the partial cation disorder has been observed in Cu_2ZnSnS_4 sample instead by a recent neutron-diffraction measurement [3].

It has been shown that the quaternary Cu_2ZnGeX_4 compounds can be obtained through cation mutation of their II–VI analogs [18]. For example, by mutating two Zn atoms in zincblende ZnSe to Cu and Ga atom, one can obtain $CuGaSe_2$ in chalcopyrite and CA structures. Further mutation of two Ga atoms in $CuGaSe_2$ to Zn and Ge atoms will form $Cu_2ZnGeSe_4$ in KS and ST structures. As listed in Table 1, GGA underestimates the band gap values for all the compounds. This is because of the fact that GGA does not consider the existence of a derivative discontinuity of the energy with respect to the number of electrons [25,26]. However, for a group of similar compounds, such as, ZnX, $CuGaX_2$ and Cu_2ZnGeX_4, this derivative discontinuity term are almost the same [25,26]. Therefore, the band gap error, i.e., the difference between GGA calculated and experimental band gap values, shall be similar for a group of similar compounds. For example, the GGA calculated and experimental [27] band gaps are 2.09 and 3.76 eV, respectively for ZnS while they are 0.78 and 2.45 eV, respectively for $CuGaS_2$. Therefore, the band gap error is 1.67 eV for ZnS which is the same as the band gap error for $CuGaS_2$. Since ZnS, $CuGaS_2$ and Cu_2ZnGeS_4 are similar compounds, the band gap error should also be 1.67 eV for Cu_2ZnGeS_4 and it can be used to correct the GGA calculated value. For example, the corrected band gap for KS–Cu_2ZnGeS_4 is 2.43 eV, as listed in Table 1, which is the GGA calculated value of 0.76 eV plus the band gap error 1.67 eV. Using this systematic correction, all the band gaps of Cu_2ZnGeX_4 in KS and ST structures have been corrected. Considering the experimental uncertainty, this correction is expected to be reliable within 0.15 eV.

The band structures for the three compounds in KS structure are shown along the T(Z) → Γ → N(A) lines in Fig. 1. We find that the band structures of all the compounds are rather comparable. The lowest conduction band (CB) is a sole band at about 1–3 eV. This is very characteristic for I_2–II–IV–VI_4 family and it is also different from that chalcopyrite CIGS and CIGSe compounds which have overlapping conduction bands [19]. The calculations indicate that the band gap decreases with the increasing anion atomic numbers [28]. For example, the band gap is 2.43 eV for KS–Cu_2ZnGeS_4 compared to 1.60 eV for KS–$Cu_2ZnGeSe_4$ and 0.81 eV for KS–$Cu_2ZnGeTe_4$. This is because the valence band maximum (VBM) is composed of hybridized Cu 3*d* and group VI *p* states. The shallower atomic level of heavy anion atom results in higher VBM states, therefore smaller band gaps. Comparison of the band structures between KS and ST structures shows that band gaps of the KS structure are in general larger than those of ST structure. This is due to the fact that the KS structure has larger anion displacements. For example, the anion displacement in $Cu_2ZnGeSe_4$ system is 0.2542 for KS structure compared to 0.2479 for ST structure [17]. The band gaps of these compounds range from 0.55 to 2.43 eV, cov-

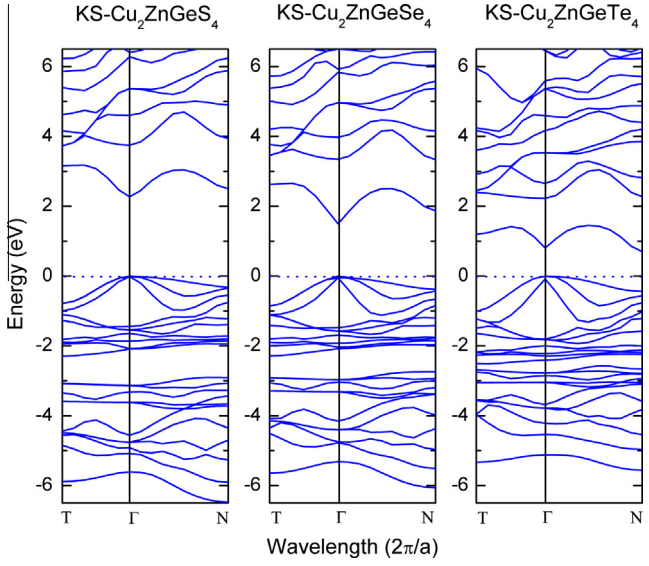

Fig. 1. Calculated band structure along the high-symmetry lines in the first Brillouin zone,: T(Z): $2\pi/a(0, 0, 0.5) \rightarrow \Gamma$:$2\pi/a(0, 0, 0) \rightarrow N(A)$:$2\pi/a$ (0.5, 0.5, 0.5), for Cu_2ZnGeS_4, $Cu_2ZnGeSe_4$ and $Cu_2ZnGeTe_4$ in KS structure.

ering a wide range of solar spectra. In particular, $Cu_2ZnSnSe_4$, with band gap values of 1.60 eV for KS and 1.32 eV for ST structure, is a potential candidate for photovoltaic applications.

The density of states (DOS) of Cu_2ZnGeS_4 in KS and ST structures, $Cu_2ZnGeSe_4$ and $Cu_2ZnGeTe_4$ in KS structure are shown in Fig. 2. From the calculated DOS, it can be clearly seen that the DOS of the KS and ST structures are quite similar. The upper VB DOS contains mainly the hybridization between *p* states from the anion atoms and 3*d* state from Cu atoms while the lower CB DOS consists mainly of the hybridization between cation *s* states and anion *p* states. Comparing the DOS between different structures and compounds, we find that: (i) the valence band width of KS structure is slightly narrower than that of the ST counterpart. This is because the KS structure has longer Cu–X (X = S, Se and Te) bonds and hence larger anion displacement than the corresponding ST structure. Therefore, the hybridization between Cu 3*d* state and anion *p* state is weaker in the KS structure, leading to a narrower band width; (ii) analyzing the band structure in Fig. 1 together with the DOS in Fig. 2 shows that the lowest solo conduction band is derived from the Ge 4*s* and anion *p* states. The conduction band shifts to the lower energy when the anion atomic number increases from S to Te; (iii) in the valence band region, from −6 eV to −2.5 eV, there are bonding states consisting of anion *p* states hybridized with Cu 3*d* state. From −2.5 eV to 0 eV, there are anti-bonding states consisting of anion *p* states hybridized with Cu 3*d* state. The overlapping (at around −2.5 eV) between the *p*–*d* bonding and anti-bonding states increases when the group VI anion atomic number increases from S to Te.

Fig. 3 gives the dielectric function $\varepsilon(\omega) = \varepsilon_1(\omega) + i\varepsilon_2(\omega)$ of all the three compounds in KS and ST structures. Overall, the three compounds show similar dielectric functions over a broad range of energy. The main difference is that the spectrum shifts to lower energy region when the anion atomic number increases. In the lower energy region, the spectrum of $Cu_2ZnGeTe_4$ compound is above the other two materials while the spectrum of Cu_2ZnGeS_4 compound is above the others in the higher energy region. The spectra exhibit some critical point (CP) structures E_{1A}, E_{1B} labeled in Fig. 3 and listed in Table 1. The E_{1A} and E_{1B} energy thresholds can be attributed to transitions at the high CPs N(A) and T(Z) of the first Brillouin zone. According to the band structures in Fig. 1, we find E_{1A} and E_{1B} are 2.99 and 4.10 eV for KS–Cu_2ZnGeS_4 while a recent ellipsometry measurement [16] shows 2.85–2.88 eV for E_{1A} and 4.03–4.34 eV for E_{1B}, as listed in Table 1. Our calculated results are in good agreement with the experimental values. It is also interesting to analyze the shift of the spectrum as a function of the anion atomic number in the three compounds. As it has been stated, the conduction band is derived from the hybridization of the Ge 4*s* and anion *p* states. When the anion atomic number increases (e.g. S → Se → Te), the Ge-X hybridization becomes higher which shifts downward the CBM, and hence the spectrum moves toward the lower energy regime.

The optical complex refractive index $\tilde{n} = n + ik$ that are of interest for the design of optoelectronic devices can be computed from dielectric functions [29]. Fig. 4 presents the energy dependent *n* and *k* values of all the three compounds in KS and ST phases. In experiment, *n* and *k* of Cu_2ZnGeS_4 in the energy range from 1.4 to 4.7 eV are reported [16]. Our calculated results are in good accord with the experimental values. For example, our calculated *n* at energy 1.4 eV is 2.68 compared to the corresponding 2.65 from experiment. The peak values from experiment at energy range of 2.4–2.9 eV is 3.02 compared to our calculated 2.97–3.18 in Fig. 4. We find that the static refractive index (n_0 in Table 1) increases from sulfide to telluride compound and increases from KS to ST structure.

In Fig. 5, we present the calculated results of the absorption coefficient α and normal incident reflectivity *R* for all the cases, which represent the linear optical response from the VBs to the lowest CBs. Due to the fact that the absorption and reflectivity are obtained from the dielectric function [29], all the compounds in this study have similar absorption spectra, although with different energy for the onset to absorption (i.e., the band gap energy). It is found that the Cu_2ZnGeS_4 compound has large band-edge absorption coefficient (about $5 \times 10^4\ cm^{-1}$). At a given photon energy, the $Cu_2ZnGeTe_4$ compound has the largest absorption coefficient while the Cu_2ZnGeS_4 compound has the smallest value. Comparison with the calculated spectra of other materials [19,30] shows that the absorption coefficient of Cu_2ZnGeX_4 is smaller than that of Cu_2ZnSnX_4 and Cu_2ZnTiX_4 has the largest

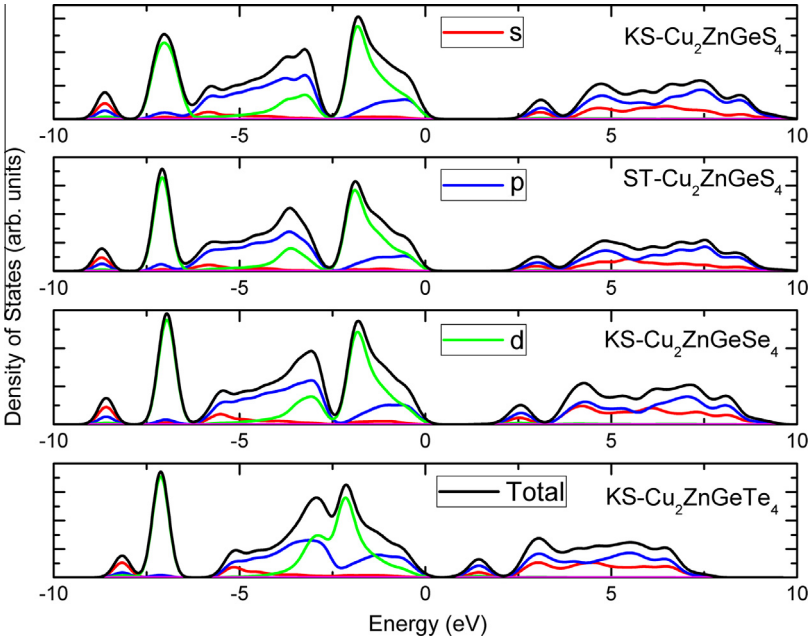

Fig. 2. The partial and total DOS of Cu_2ZnGeS_4 in KS and ST structures, $Cu_2ZnGeSe_4$ and $Cu_2ZnGeTe_4$ in KS structure.

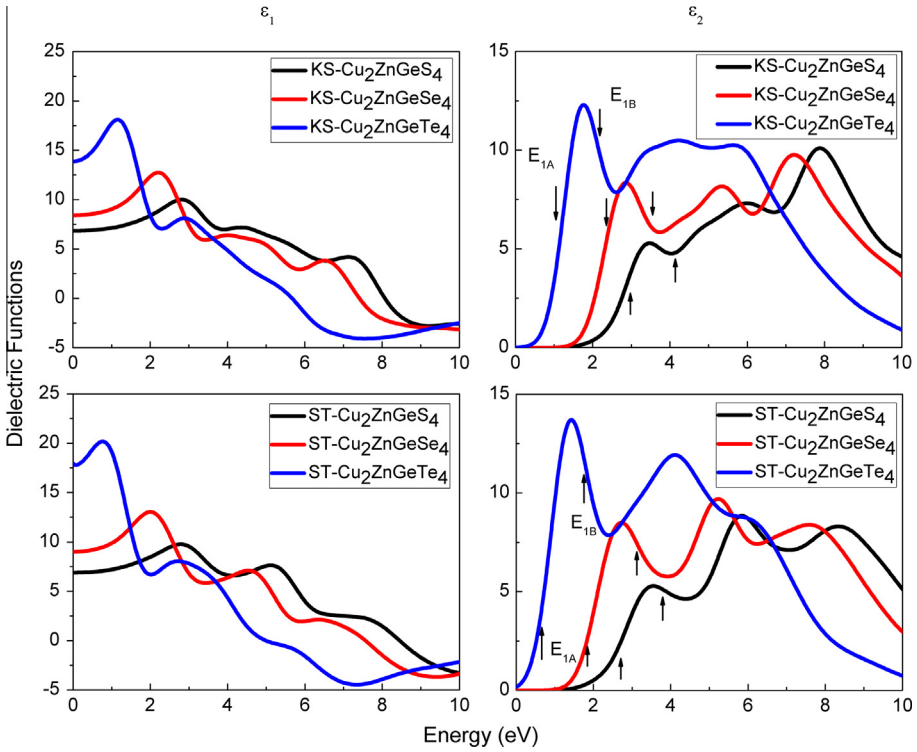

Fig. 3. The dielectric function $\varepsilon(\omega) = \varepsilon_1(\omega) + i\varepsilon_2(\omega)$ of Cu_2ZnGeS_4, $Cu_2ZnGeSe_4$ and $Cu_2ZnGeTe_4$ in KS and ST structures. The left panels represent the real part $\varepsilon_1(\omega)$ and the right panels represent the imaginary part $\varepsilon_2(\omega)$. The optical transitions E_{1A} and E_{1B} are labeled in the $\varepsilon_2(\omega)$ spectra.

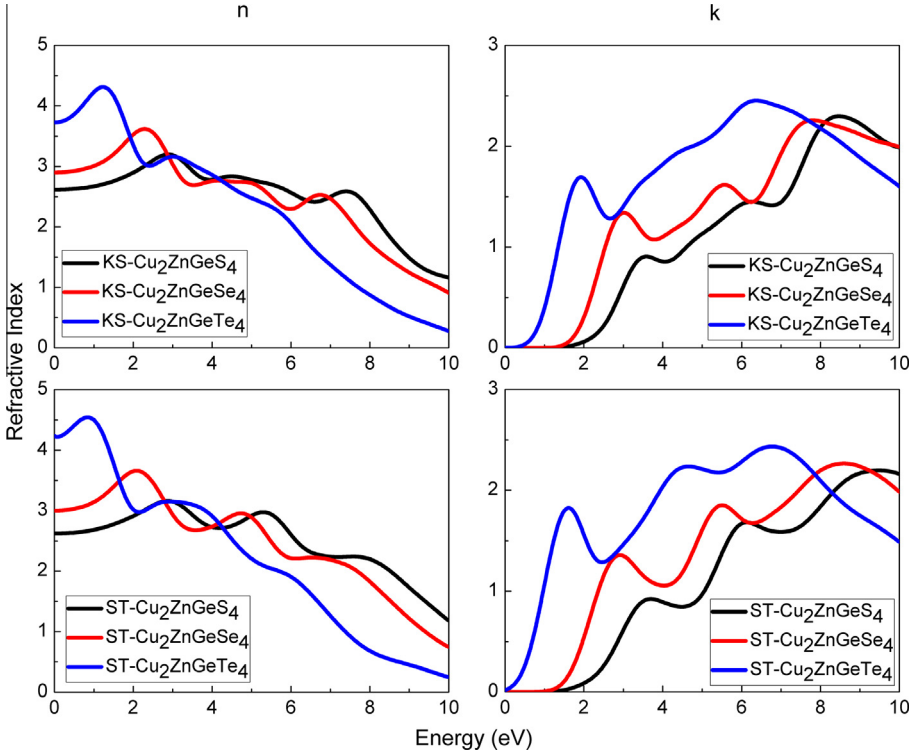

Fig. 4. The complex refractive index of Cu_2ZnGeS_4, $Cu_2ZnGeSe_4$ and $Cu_2ZnGeTe_4$ in KS and ST structures. The left panels represent the refractive index n and the right panels represent the extinction coefficient k.

absorption coefficient. This might indicates that the compounds with heavier group IV elements should have higher light transformation efficiency. It is noticed that, at energy range of 1.5–4.0 eV, the reflectivity and absorption coefficient decreases for all the compounds. We find this energy region corresponds to the gap between the lowest solo CB and the upper CBs of the band structures

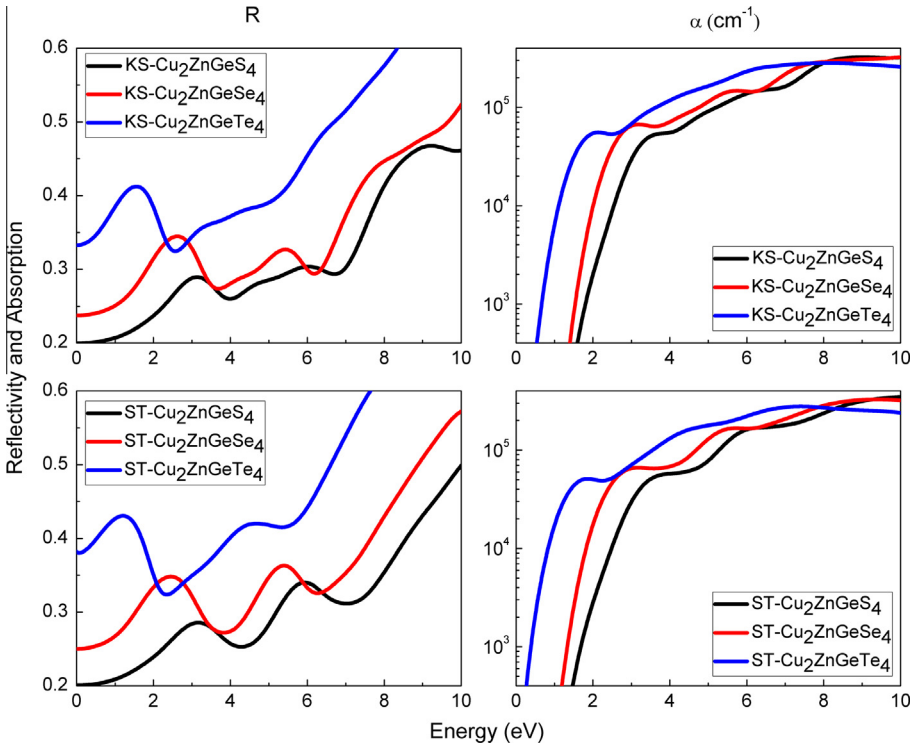

Fig. 5. The normal incident reflectivity and absorption coefficient of Cu_2ZnGeS_4, $Cu_2ZnGeSe_4$ and $Cu_2ZnGeTe_4$ in KS and ST structures. The left panels represent the reflectivity R and the right panels represent the absorption coefficient α (cm^{-1}). The absorption coefficient is plotted in logarithm scale.

in Fig. 1. Since the upper CBs do not contribute to the optical absorption in the low energy regime. This conduction band gap is a disadvantage for the band-edge absorption efficiency in KS and ST structures.

4. Conclusion

In conclusion, using first-principles density functional methods, we have studied the electronic and optical properties of Cu_2ZnGeS_4, $Cu_2ZnGeSe_4$ and $Cu_2ZnGeTe_4$ in KS and ST structures. Band structures and optical spectra such as the dielectric function, refractive index, absorption coefficient and reflectivity have been determined. We find that the conduction band shifts downward and the overlapping between p–d bonding and anti-bonding states in the valence band increases when the system changes from Cu_2ZnGeS_4 to $Cu_2ZnGeSe_4$ and then $Cu_2ZnGeTe_4$. Some critical points in the optical spectra are assigned to the interband transitions according to the calculated band structures. The electronic structures and optical spectra are rather similar in shape for all the compounds. When anion atomic number increases from S to Te, the optical spectra shift to the low energy regime. A good agreement between our calculated results and the experimental data has been obtained.

References

[1] P.A. Fernandes, P.M.P. Salome, A.F. da Cunha, J. Alloys Comp. 509 (2011) 7600.
[2] A. Shavel, J. Arbiol, A. Cabot, J. Am. Chem. Soc. 132 (2010) 4514.
[3] S. Schorr, H.J. Hoebler, M. Tovar, Eur. J. Mineral. 19 (2009) 65.
[4] H. Katagiri, K. Jimbo, S. Yamada, T. Kamimura, W.S. Maw, T. Fukano, T. Ito, T. Motohiro, Appl. Phys. Express 1 (2008) 041201.
[5] A.V. Moholkar, S.S. Shinde, A.R. Babar, K. Sim, H.K. Lee, K.Y. Rajpure, P.S. Patil, C.H. Bhosale, J.H. Kim, J. Alloys Comp. 509 (2011) 7439.
[6] T.K. Todorov, K.B. Reuter, D.B. Mitzi, Adv. Mater. 22 (2010) E156.
[7] M.L. Liu, I.W. Chen, F.Q. Huang, L.D. Chen, Adv. Mater. 21 (2009) 3808.
[8] C. Sevik, T. Cagin, Phys. Rev. B 82 (2010) 045202.
[9] K. Doverspike, K. Dwight, A. Wold, Chem. Mater. 2 (1989) 194.
[10] H. Matsushita, T. Maeda, A. Katsui, T. Takizawa, J. Cryst. Growth 208 (2000) 416.
[11] O.V. Parasyuk, I.D. Olekseyuk, L.V. Piskach, J. Alloys Comp. 397 (2010) 169.
[12] H. Matsushita, T. Ichikawa, A. Katsui, J. Mater. Sci. 40 (2005) 2003.
[13] O.V. Parasyuk, L.V. Piskach, Y.E. Romanyuk, I.D. Olekseyuk, V.I. Zaremba, V.I. Pekhnyo, J. Alloys Comp. 397 (2005) 85.
[14] G.Q. Yao, H.S. Shen, E.D. Honig, R. Kershaw, K. Dwight, A. Wold, Solid State Ionics 24 (1987) 249.
[15] D.M. Schleich, A. Wold, Mater. Res. Bull. 12 (1977) 111.
[16] M. Leon, S. Levcenko, R. Serna, G. Gurieva, A. Nateprov, J.M. Merino, E.J. Friedrich, U. Fillat, S. Schorr, E. Arushanov, J. Appl. Phys. 108 (2010) 093502.
[17] Y. Zhang, X. Sun, P. Zhang, X. Yuan, F. Huang, W. Zhang, J. Appl. Phys. 111 (2012) 063709.
[18] S. Chen, X.G. Gong, A. Walsh, S.H. Wei, Phys. Rev. B 79 (2009) 165211.
[19] C. Persson, J. Appl. Phys. 107 (2010) 053710.
[20] M.C. Payne, M.P. Teter, D.C. Allan, T.A. Arias, J.D. Joannopoulos, Rev. Mod. Phys. 64 (1992) 1045.
[21] D. Chen, N.M. Ravindra, Emerg. Mater. Res. 2 (2) (2013) 109.
[22] J.P. Perdew, K. Burke, M. Ernzerhof, Phys. Rev. Lett. 77 (1996) 3865.
[23] D. Vanderbilt, Phys. Rev. B 41 (1990) 7892.
[24] G.S. Babu, Y.B.K. Kumar, P.U. Bhaskar, V.S. Raja, Semicond. Sci. Technol. 51 (1983) 1884.
[25] J.P. Perdew, M. Levy, Phys. Rev. Lett. 51 (1983) 1884.
[26] P. Mori-Sanchez, A.J. Cohen, W. Yang, Phys. Rev. Lett. 100 (2008) 146401.
[27] O. Madelung, Semiconductors: Data Handbook, third ed., Springer, Berlin, 2004.
[28] D. Chen, N.M. Ravindra, J. Mater. Sci. 47 (2012) 5735.
[29] C. Lamsal, D. Chen, N.M. Ravindra, TMS Proc. 1 (2012) 701.
[30] X. Wang, J. Li, Z. Zhao, S. Huang, W. Xie, J. Appl. Phys. 112 (2012) 023701.